2017 International Nuclear Atlantic Conference - INAC 2017
Belo Horizonte, MG, Brazil, October 22-27, 2017
ASSOCIAÇÃO BRASILEIRA DE ENERGIA NUCLEAR – ABEN

Agência Brasileira do ISBN
ISBN 978-85-99141-07-6
9 788599 141076

SIMULATION OF ACCIDENT-TOLERANT U_3Si_2 FUEL USING FRAPCON CODE

Daniel S. Gomes[1], Antonio T. Silva[1], Alfredo Y. Abe[1], Rafael O. R. Muniz[1], Claudia Giovedi[2]

[1] Instituto de Pesquisas Energéticas e Nucleares (IPEN / CNEN - SP)
Av. Professor Lineu Prestes 2242
05508-000 São Paulo, SP
dsgomes@ipen.br, teixeira@ipen.br, alfredo@ctmsp.mar.mil.br, rafael.orm@gmail.com

[2] Universidade de São Paulo Departamento de Engenharia Naval e Oceânica
Av. Prof. Mello Moraes 2231
05508-000 São Paulo, SP
claudia.giovedi@ctmsp.mar.mil.br

ABSTRACT

The research on accident-tolerant fuels (ATFs) increased after the Fukushima event. This benefitted risk management in nuclear operations. In this investigation, the physical properties of the materials being developed for the ATF program were compared with those of the standard UO_2–Zr fuel system. The research efforts in innovative fuel design include rigorous characterization of thermal, mechanical, and chemical assessment, with the objectives of making the burnup cycle longer, increasing power density, and improving safety performance. Fuels must reach a high uranium density—above that supported by UO_2—and possess coating that exhibits better oxidation resistance than Zircaloy. The uranium density and thermal conductivity of ATFs, such as U_3Si_2, UN, and UC, is higher than that of UO_2; their combination with advanced cladding provides possible fuel–cladding options. An ideal combination of fuel and cladding must increase fuel performance in loss-of-coolant scenarios. The disadvantages of U_3Si_2, UN, and UC are their swelling rates, which are higher than that of UO_2. The thermal conductivities of ATFs are approximately four times higher than that of UO_2. To prevent the generation of hydrogen due to oxidation of zirconium-based alloys in contact with steam, cladding options, such as ferritic alloys, were studied. It was verified that FeCrAl alloys and SiC provide better response under severe conditions because of their thermophysical properties. The findings of this study indicate that U_3Si_2 and the FeCrAl fuel cladding concept should replace UO_2–Zr as the fuel system of choice.

1. INTRODUCTION

Following the Fukushima Daiichi nuclear disaster, efforts have been directed toward the development of the accident tolerant fuel (ATF) concept. Advanced fuels can reduce disaster risk for the next generation of reactors. The ATF campaign has led to studies on advanced fuels in the current phase between Gen-III and Gen-IV reactors. Innovative fuels should improve fuel management and plant safety and reduce costs. ATFs will permit more extended fuel cycles and reduce waste, improving efficiency and safety. Advanced fuels must replace the current UO_2–Zr system. High thermal gradients are produced inside UO_2 pellets; this weakens the ceramic structure and increases incident risk [1]. For a standard fuel system that works at a peak linear power rate of 45 kW/m, fuel centerline temperatures can reach over 1400 °C. In addition, the thermal conductivities of several ATF candidates, such as U_3Si_2, UC, and UN, are

approximately four times higher than that of UO_2. Cladding must be designed to prevent hydrogen explosion in a loss-of-coolant accident [2]. Claddings based on iron–chromium–aluminum (FeCrAl) have potential for replacing Zircaloy. The oxidation rates of zirconium alloys are hundred orders of magnitude higher than those of FeCrAl [3].

1.1 Accident Tolerant Fuel Concept

New fuels were developed under the ATF program. The basic idea was to improve safety margins and fuel management. These fuels exhibit increased uranium loading, with an enrichment of 5%. In addition, these fuels exhibit higher thermal conductivity, which may lead to lower temperatures than those generated by UO_2. All these properties can provide longer burn cycles and reduce cost. The enrichment of U_3Si_2 fuel is 15% less than that of UO_2. UN and UC exhibit high melting points of 2395 °C and 2886 °C, respectively, and they are the targets of study in the ATF program [4]. A key factor is referring to the potential water reaction, which produces hydrogen. Earlier, binary UC and mixed uranium–plutonium carbide were used in fast breeder reactors. A tolerant UC fuel with SiC as cladding was studied in the ATF program. Currently, has led to the consideration of FeCrAl ternary alloy as advanced cladding [5]. The properties of various fuels are compared in Table 1.

Table 1: Properties of tolerant fuels candidates to replace UO_2

Tolerant fuel	Specific density (g/cm^3)	Uranium density (gU/cm^3)	Melting point (°C)	Thermal conductivity (W/m-K)	Irradiation induced swelling
U_3Si_2	11.31	12.2	1665	16.3	Medium
U_3Si	15.4	14.8	985	20.0	Medium
UO_2	10.86	9.66	2840	4.6	Low
UN	14.33	13.50	2850	20.9	Medium
UC	13.63	12.97	2507	20.0	High

1.2 ATF Guidelines

The guideline proposed by DOE provides general steps for assessing the performance of accident-tolerant fuels. In the first step, the enhanced behavior of a fuel rod is analyzed. The fuel system based on UO_2/Zr alloys must improve safety under steady state, due to a reduction in a temperature of operation. The average fuel temperature must exhibit low corrosion rates, reduce assisted cracking, and prevent hydrogen effect produced in zirconium alloys. In this manner, an ATF must provide a better fuel response than UO_2 and zirconium alloys under transient conditions. During accidents, fuel rod reaches temperatures from 400 °C to 1200 °C that help to produce fuel failures U_3Si_2–FeCrAl is an ATF concept that enhances fuel response and diminishes risk. Fuel behavior during a severe accident should prevent the effects of hydrogen, generation as compared with a classical system. The guideline recommends reduced production of hydrogen owing to oxidation to prevent the explosion of hydrogen gas. Next, metallurgical processes are defined and applied to the fuel concept to provide economic benefits and to make fabrication processes easy and inexpensive. In the next step, the storage conditions of spent fuel are described. Spent fuel can be transferred to a dry cask, where it can be stored for periods of the order of 100 years before disposition at a nuclear waste site.

1.3 Licensing Fuel Code

The steady state and transient simulations of a single fuel rod were performed using fuel codes FRAPCON and FRAPTRAN. These codes are computational tools for evaluating fuel performance during normal and off-normal situations. FRAPCON calculates the steady state response of light water reactor fuel rods during long-term burns [6]. In parallel, FRAPTRAN can analyze the performance of a fuel rod during a transient state as loss-of-coolant accident (LOCA). In this study, the response of U_3Si_2 was simulated using a fuel performance code and applied to a fuel rod tested under The Halden Project. The response of U_3Si_2 can be simulated by including the physical properties of U_3Si_2 in the source code can reproducing fuel behavior using FRAPCON. The new system version enables FRAPCON to predict the fuel performance associated with advanced fuel/cladding systems based on U_3Si_2–Zr alloys and U_3Si_2–FeCrAl.

2 TEORETHICAL BACKGROUND

2.1 Physical Models

The routines adapted to the fuel code must represent all thermochemical properties of U_3Si_2. Moreover, key physical models that can represent the performance of U_3Si_2 were included in FRAPCON. Mechanical behavior is calculated as function of thermal expansion, specific heat, and conductivity. Tolerant fuels exhibit better output parameters than UO_2, such as centerline temperature and hoop stress. Owing to the thermal response of U_3Si_2, the fuel centerline temperature working with power of 45 KW/m can remain approximately 400° lower than that of UO_2. Moreover, the average temperature of the U_3Si_2 pellet when a linear heat generation rate of 45 KW/m is applied must reduce to up to 160 °C.

2.2 Uranium Silicide Pellet Fabrication

U_3Si_2 pellets are produced using a mixture of powders composed of silicon and uranium. A compact agglomerate is created and sent to a furnace at 1450 °C, followed by an arc melter. In the arc melter, uranium reacts with silicon to produce U_3Si_2 with a purity of 97%. Then, the U_3Si_2 ingot is comminuted into a fine powder and pressed to form a green pellet under approximately 138 MPa. Next, sintering is performed for approximately 4 hours at 1500 °C. This manufacturing process has several challenges; for example, the sizes of the particles in the fine powder range from 1 µm to 10 µm. The high density of U_3Si_2 complicates the grinding process. All safety rules associated with the fabrication processes that use radioactive uranium must be followed [7].

2.3 Thermal Conductivity

In general, irradiated ceramic fuels exhibit a phenomenon that may help in describing their thermal conductivity. In a temperature range of 400 °C to 1200 °C, the thermal conductivity of U_3Si_2 (13 to 22 W/m-K) is higher than that of UO_2 (6 to 2.5 W/m-K) [8]. Among the advantages of ATFs, lower operating temperatures are considerably safer when SiC or FeCrAl claddings are used. The theoretical model of thermal conductivity expresses it as a function of adjustable factors. Equation (1) expresses the thermal conductivity of UO_2 as a function of temperature (K), burnup (GWd/MTU), and fuel porosity (%) [9]. Equation (2) shows the correction factor used for fuel porosity.

$$k(UO_2) = F \times \{(0.040 + 2.57 \times 10^{-4} T)^{-1} + 72.6 \times 10^{-12} T^3\} \quad (1)$$

$$F = 1 - 2.5P \quad (2)$$

where P denotes porosity; P = 0.05 for UO_2 with a density/theoretical density of 95%; T represents temperature in K. Equation (3) shows the thermal conductivity of U_3Si_2 for its monolithic form as a function of temperature; this equation is valid from 293.15 K to 1473.15 K [10].

$$k(U_3Si_2) = 6.5869 - 0.0051 * T \quad (3)$$

In general, the thermal conductivity of tolerant fuels may increase as a function of temperature. However, the thermal conductivity of UN is higher than that of U_3Si_2. In the case of an accident, when temperatures can vary from 800 °C to 1200 °C, the thermal conductivity of U_3Si_2 reaches 14 W/m-K on average. Under the same condition, the thermal conductivity of UN is considerably higher at approximately 20 W/m-K [11].

2.4 Thermal Expansion

The coefficients of U_3Si_2 are calculated based on the tests carried out at Los Alamos National Laboratory. The thermal linear expansion of U3Si2 is described by Eq. (4), which is valid from 293.15 K to 1223.15 K. The thermal expansion strain data for U3Si2 were considered for temperatures of up to 1273 K under a 10 ppm O2 argon gas stream. Equation (5) shows thermal expansion strain as a function of temperature (K); the equation is valid up 1273 K [8], [11].

$$cte(U_3Si_2) = -0.002T + 16.25 \quad (4)$$

$$\frac{dL}{L_0}(U_3Si_2) = 1.518 \times 10^{-5} T - 4.054 \times 10^{-4} \quad (5)$$

2.5 Heat Capacity and Enthalpy

The specific heat of innovative fuels is less than that of UO_2. The heat capacity of U_3Si_2 at fuel temperature could reduce the energy stored in fuel. There is a slight equivalence between the specific heats of U_3Si_2 and UO_2 in a range of 1226 °C to 1665 °C. However, the specific heat of UC is slightly higher than that of UN below 2273 °C. The specific heat, *Cp* (J/kg-K), used for U_3Si_2 is an empirical correlation obtained from stoichiometric U_3Si and USi alloys, at 6.1 wt% silicon. Early studies frequently do not specify a temperature range for applying this expression. However, the expression is well accepted for evaluating specific heat at temperatures below 900 K. If the correlation represents a line, we extrapolate it to high temperatures. Equations (6), (7), and (8) show the specific heats of UO_2, U_3Si_2, and U_3Si, respectively [8], [11].

$$Cp(UO_2) = \frac{K_1 \exp(\theta / T)}{T^2 [\exp(\theta / T - 1]^2} + K_2 T + \left(\frac{O/M}{2} \right) \frac{K_3 E_D}{RT^2} \exp(-E_D / RT) \quad (6)$$

$$Cp(U_3Si_2) = 199 + 0.019 \times (T - 273.15) \quad (7)$$

$$Cp(U_3Si) = 171 + 0.019 \times (T - 273.15) \quad (8)$$

where Cp (J/kg-K) denotes specific heat, temperature is in K, K_1 = 296.7, $K_2 = 2.43 \times 10^{-2}$, $K_3 = 8.75 \times 10^7$, θ = 535.285, and $E_D = 1.577 \times 10^5$.

The correlations used for enthalpy and heat capacity are functions of temperature, fuel composition, O/M ratio, and burn cycle. Both properties may increase with temperature. The enthalpy of pellet fuel relative to its enthalpy at 273.15 K can be obtained by integrating heat capacity. The enthalpy of fuel is 10–25% less than the total energy calculated under a power burst phase. The first limit proposed was 280 cal/g. This threshold, which is defined for fresh fuels, limits the radial average enthalpy under a reactivity-initiated accident. Equations (9) and (10) express the enthalpies of UO_2 and U_3Si_2, respectively [8], [9], [11].

$$H(UO_2) = \frac{K_1\theta}{\exp^{(\theta/T)} - 1} + \frac{K_2T^2}{2} + \frac{(O/M)}{2}\{K_3 \exp^{(-E_D/(RT)}\} \quad (9)$$

$$H(U_3Si_2) = 0.0095T^2 + 198.481T \quad (10)$$

where H (J/kg) denotes fuel enthalpy, temperature is in K, and the values of constants K_1, K_2, K_3, and E_D are the same as those used for specific heat.

2.6 Swelling

Nuclear fuels swell when they are irradiated, depending on fission rate and temperature. Fission releases noble gases, such as xenon and krypton, and adds solid products to crystal structure. Fuel codes can divide swelling into two models to calculate solid and gaseous fission products. Experimental data were used to develop a swelling model for U_3Si_2/Al to build a theoretical basis [12]. The results were applied in part to predict the response of the fuel plates used in the research reactors. The models for U_3Si_2 pellet fuels are based on the data obtained from irradiation tests. The swelling strain of monolithic fuel was calculated using the results of miniplate irradiation tests. If the theoretical density of U_3Si_2 was 95%, with a uranium density of 10,735 gU/cm^3, a correlation was obtained as a function of burnup. Equation (11) shows a formulation used to estimate the swelling of U_3Si_2. The strain created in the inner pellet owing to volumetric swelling is calculated as function of burnup, as shown in Eq. (12) [8], [11].

$$\left(\frac{V}{V_0}\right)_{gas} = 3.88008 * Bu^2 + 0.79811 * Bu \quad (11)$$

$$\left(\frac{V}{V_0}\right)_{solid} = 0.94519 * Bu \quad (12)$$

Earlier, several irradiation tests were performed in a test reactor using forms of uranium and silicon such as USi_2, USi, and U_3Si_2. The swelling rate of these forms was higher than that of UO_2 [12].

Applying the model described in Eq. (13), it is noted that the swelling of U_3Si_2 can be twice that of UO_2 for burn cycles over 60 GWd/MTU. Volumetric strain is the first derivative of the swelling correlation; it is an artifice used in performance codes. Equation (13) describes the volumetric strain developed in the pellet owing to the deformation due to swelling [11], [13].

$$\frac{d(V/Vo)}{dBu} = 7.76016 * Bu + 0.79811 \tag{13}$$

2.7 Densification Models

Uranium silicide fuel exhibits densification at the start of the burn cycle below 20 GWd/ MTU; this is characterized as the reverse of the swelling due to irradiation. UO_2 and U_3Si_2 exhibit similar densification. The densification process has a strong influence on reducing pore size when fuel is irradiated to create a small porosity fraction. For smaller pore sizes, the gaps with less gap conductance increase, heat transfer decreases, and cladding may collapse. Equations (14) and (15) describe the densification model [8], [11].

$$\varepsilon_D = \Delta\rho_0 (e^{(Bu * \ln(0.01)/C_D Bu_D)} - 1) \tag{14}$$

For temperatures below 750 °C, parameter C_D is given by Eq. (14), and it is equal to 1 at a temperature of above 750 °C.

$$C_D = 7.2 - 0.0086(T - 25) \tag{15}$$

where ε_D denotes densification strain, $\Delta\rho_0$ represents full densification, and Bu denotes the burnup level. For temperatures below 1023.15 K, parameter C_D is given by Eq. (15), and it is equal to 1 above 1023.15 K.

2.8 Iron–Chromium–Aluminum Alloy

Previously, using austenitic steel as cladding was a good option because steel is easy and inexpensive to manufacture. However, exist a vast experience gained the neutron cross section of steel showed ten magnitude order over Zircaloy. Stainless steel requires a thinner wall to compensate for the impact of the neutron absorption cross section. The stainless-steel melts at a slightly low temperature (approximately 1450 °C), and it is susceptible to stress corrosion cracking [12]. The ATF program investigated cladding concepts that could prevent hydrogen detonation under accident conditions. Hydrogen explosion due to the steam reaction is the key consequence due to fuel failure as occurred in the Fukushima disaster, 2011 [13].

The ferritc alloys show the typical tensile behavior expected from ferritic steels. Uniform elongation is >20% at room temperature and 300°C. Oxide dispersion strengthened (ODS) FeCrAl alloys are being developed with optimum composition and properties for accident tolerant fuel cladding. Ideally, a cladding concept should improve reaction kinetics with steam, lead to slower hydrogen generation. Also, must improve mechanical properties compared to zirconium alloys [14]. FeCrAl alloy system combined with U_3Si_2 has the great potential to develop advanced fuel systems. The experience acquired on ferritic Fe-Cr based alloys has possible instabilities in the micro structure, under neutron irradiation [15]. Table 2, shows the physical properties of a few alloys that were investigated.

Table 2: Fuel cladding material properties at room temperature

Advanced cladding materials	Density (g/cm^3)	Cross section (barns)	Young modulus (GPa)	Yield Strength (MPa)	Thermal conductivity (W/m-k)	Coefficient of thermal expansion ($10^{-6}m/°C$)
Zircaloy	6.56	0.20	94.5	230	16.7	6
FeCrAl	7.1	2.43	220	460	11.0	12.5
APMT	7.3	2.47	220	540	11.0	12.4
304SS	7.9	2.88	200	515	16.2	17.3
310SS	8.03	0.806	200	310	14.2	15.8

FeCrAl alloys exhibit an elasticity modulus of 151 GPa and a Poisson's ratio 0.3 under steady state at temperatures of 350 °C. The Young's modulus of the MA956 alloy composed of Fe–20Cr–4.5Al (wt %) (160–151 GPa) was higher than that for Zr-4 (81–75 GPa). Equations (16) and (17) express the elastic moduli of the KANTAL and MA956 alloys, respectively [16].

$$E(KANTHAL) = 1.92 \times 10^{-5} T^2 - 0.06041 T + 237 \quad (16)$$

$$E(MA956) = -3.2 \times 10^{-5} T^2 - 0.04497 T + 190.6 \quad (17)$$

The thermal conductivities of FeCrAl alloys below 600 K range from 10–15 W/m-K, which is 15% less than that of Zr-4. For temperatures ranging from 600 K–1300 K, the thermal conductivity of KANTHAL-APMT varies from 15 to 27 W/M-K, which is10% less than that of Zr-4. Equations (18) and (19) express the coefficients of thermal expansion of the KANTAL and MA956 alloys, respectively [17].

$$cte(KANTHAL) = 0.01638 T + 5.236 \quad (18)$$

$$cte(MA956) = 0.005236 T + 9.259 \quad (19)$$

Zircaloy exhibits lower heat capacity than FeCrAl alloys. High specific heat can improve fuel safety by introducing a slower transient response. Under normal operation, the specific heats of Zircaloy and FeCrAl vary from 306–317 J/kg-K and 574–609 J/kg-K, respectively. Equations (20) and (21) express the heat capacities of the KANTAL and MA956 alloys, respectively [11].

$$Cp(KANTHAL) = 0.0001912 T^2 - 0.5848 T + 322.2 \quad (20)$$

$$Cp(MA956) = 0.2779 T + 387.5 \quad (21)$$

3.0 FUEL ROD SIMULATION

In this investigation, we implemented new capacities for the licensing code, FRAPCON. The system code was modified to simulate advanced fuels including U_3Si_2/FeCrAL option. The advanced versions comprised all thermal properties, swelling models, and creep rate equations.

The capacity of the code to simulate the advanced fuel concept was enhanced using versions adapted to U_3Si_2, and FeCrAl. The performance of these fuels was compared with that of the UO_2–Zr fuel system. Also, other experiments were realized to verify the reduction of centerline temperature of fuel. The cladding thickness used to FeCrAl was 0.5281 mm, had a reduction compared with zirconium alloys, but maintain the same radial gap. The enrichment of U_3S_{i2} fuel can be reduced of 15%, when used with zirconium alloys due to higher uranium load. Table 3, presents fuel parameters used in simulation.

Table 3: Parameters of fuel rod simulation UO_2/Zr

Fuel parameters	UO_2
Cladding material	Zircaloy-4
Cladding outside diameter (mm)	10.735
Cladding thickness (mm)	0.721
Radial pellet gap (mm)	0,0805
Fuel grain size (μm)	10
Pellet outside diameter (mm)	9.13
Pellet length (mm)	11
Dish depth (mm)	0.28
Theoretical density UO_2 (% TD)	94.8
Burnup (GWd/MTU)	83
Fuel enrichment (%)	3.5
Fill gas pressure (MPa)	4.0
Fill gas composition	(90%Ar, 10%He)

The fuel rod simulation maintains typical operation under extended burn cycle, working under normal operation. The system code adapted to system U_3Si_2/FeCrAl was compared with fuel system UO_2/Zr. Fig. 1, presents the average power and fuel temperature for UO_2/Zr system

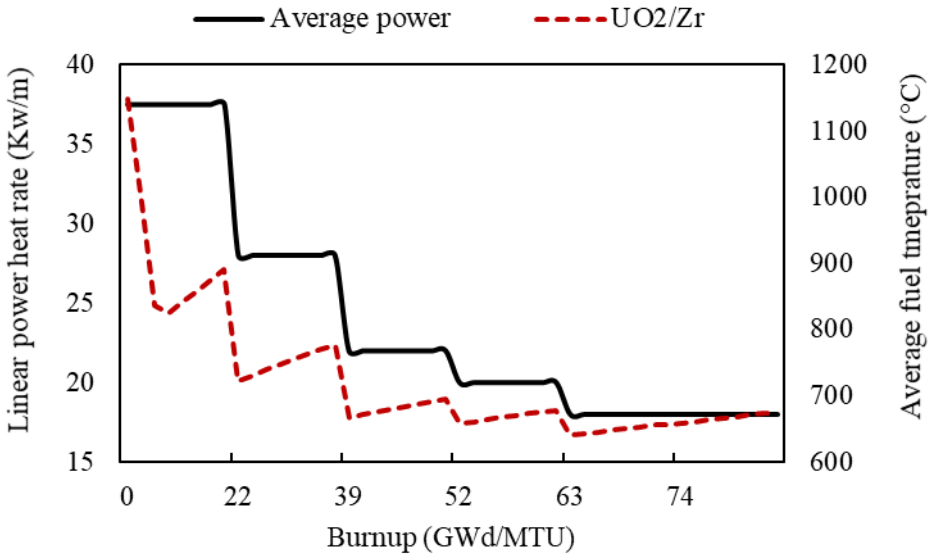

Figure 1: Average power used in simulation

In this case, the burn cycle reaches 83 GWd/MTU, which is above the recommended value by international regulators. First create a simulation using Zircaloy-4 (Sn%1.53; Fe%0.22) to compare with U_3SI_2/FeCrAl system. The power profile strongly influences the mechanical properties because of the achieved temperature**.** The irradiation cycle induces a sequence of effects, such as the loss of mechanical characteristics in the fuel. Theoretically experiment shows embrittlement due to hydrogen uptake of approximately 650 ppm that occurred due to oxidation at high temperatures and irradiation effects. The fuel centerline temperature suffered a considerable reduction as shown in Fig 2.

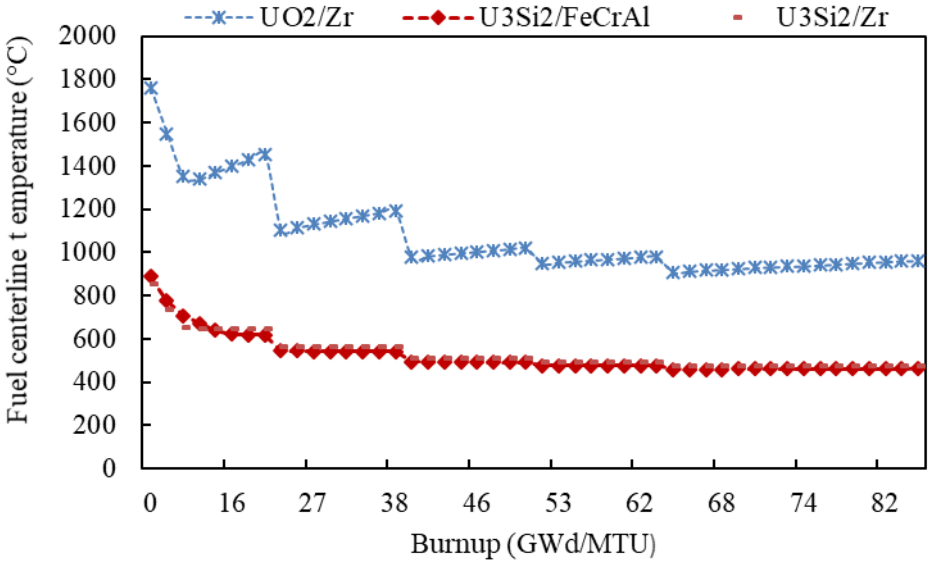

Figure 2: Fuel centerline temperature to UO_2/Zr, U_3Si_2/Zr, U_3Si_2/FeCrAl

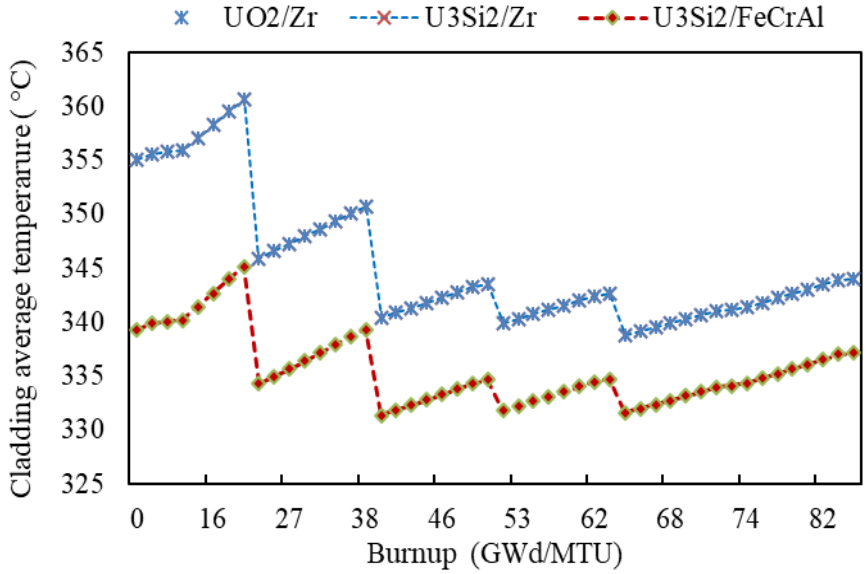

Figure 3: Cladding average temperature to UO_2/Zr, U_3Si_2/Zr, U_3Si_2/FeCrAl

Due to the high swelling rate of U_3Si_2 it should produce an increase in the volumetric deformation of the pellet causing greater stress and strain on the fuel rod. Investigation indicated that U_3Si_2 is more susceptible to chemical reaction than is UO_2. The system U_3Si_2/Zr appointed to creation of an interaction layer between Zircaloy and U_3Si_2. Undesirable effects

are disadvantages of U_3Si_2. However, the use of advanced cladding significantly reduces oxidation. Uranium silicide can show an expressive swelling rate and fission gas release correlated, that is an uncertainty source about the amount of fission gas produced by fission fuel. The higher thermal conductivity of the U_3Si_2 that can create greater tolerance to the overheating of the fuel. In table 4, showed trend of U_3Si_2/FeCrAl compared with UO_2/Zr.

Table 4 Trends of fuel systems simulated

Failure Mechanisms	UO_2/Zr	U_3Si_2/Zr	U_3Si_2/FeCrAl
Cladding designs stress	Standard	Worse	Better
Cladding designs strain	Standard	Worse	Better
Cladding fatigue	Standard	Worse	Better
Cladding oxidation	Standard	Standard	Better
Cladding collapse	Standard	Standard	Somewhat better
Fuel overheat	Standard	Better	Better

The thermal gradients created within of fuel pellet are more significant in the fuel centerline than outside surface, shown in the Fig. 3. However, these values are dependent on the linear power applied as a function of this. Also, we can verify that the external temperature undergoes a small variation for distinct systems. Exist great potential safety advantages of FeCrAl over Zircaloy for the cladding of fuel rods during LWR severe accident condition.

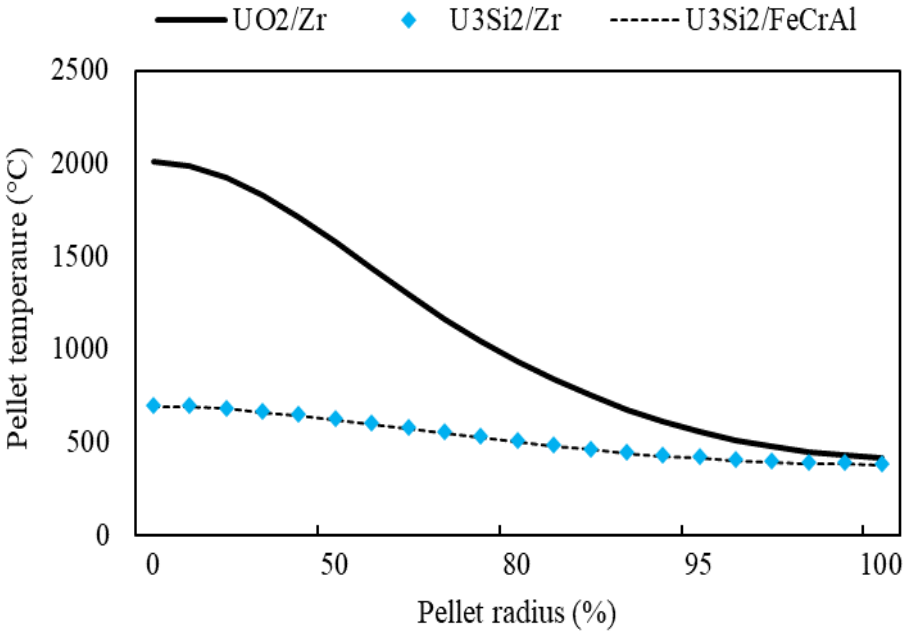

Figure 3 Radial temperature distribution inner fuel pellet

4. CONCLUSIONS

This study available the proposed advanced fuel system: U_3Si_2/FeCrAl and measure thermal response under normal operation. The simulation indicated the effects of properties include in

FRAPCON code, to analyze of fuel performance. However, the effects of swelling rate are parameters that can be reduced in next future. U_3Si_2 has advantageous enhanced thermal conductivity. Coupled with lower heat capacity and a melting point of 1665 °C. U_3Si_2 shows the heat capacity increased linearly with temperature and is consistent with thermodynamic databases in the literature. Also, metallic thermal conduction increases linearly with temperature. Theoretically, fuel enrichment could reduce, when used with zirconium alloys, but FeCrAL shows a neutron penalty, used with reduced thickness cladding to avoid power. The wall thickness for the predominantly iron-based cladding materials was assumed to be 0.0419 cm versus 0.0572 cm for zirconium alloys. The swelling rate produces a greater strain inner U_3Si_2 pellet than UO_2.The use of an advanced coating like FeCrAL alloys should avoid hydrogen formed at high temperatures, and reduce the embrittle of the cladding. Currently, there is an effort to develop advanced fuel system based on U_3Si_2. The experiment performed using U_3Si_5/Kanthal fuel concept is to shield the nitride phase from the water. UN-10%U3Si2 composite fuel system used with Kanthal-AF can reduce centerline temperature of 1650 °C for an average power of 28 KW/m. The UN-U_3Si_5/SS304 can be candidates in next future for accident tolerant fuels. Also, have investigation based on UN/U_3Si_2/UB_4, where UB_4 works as a burnable poison.

ACKNOWLEDGMENTS

This research was possible due to the support offered by the Nuclear Energy Research Institute (Instituto de Pesquisas Energéticas e Nucleares; IPEN), associated with the National Nuclear Energy Commission (Comissão Nacional de Energia Nuclear; CNEN).

REFERENCES

1. J. M., Harp, P. A., Lessing, B. H., Park, J., Maupin, “Preliminary Investigation of Candidate Materials for Use in Accident Resistant Fuel,” *LWR Fuel Performance Meeting/Top Fuel 2013* (2013).
2. T. Besmann, S. Voit, “Thermodynamic Assessment of Accident Tolerant Composite Fuel Candidate Systems,” *Advanced Fuels Campaign FY2014 Accomplishments Report* (2014).
3. R. B., Rebak, K. A., Terrani, R. M., Fawcett, "FeCrAl Alloys for Accident Tolerant Fuel Cladding in Light Water Reactors," *Proceedings of the ASME 2016 Pressure Vessels and Piping Conference* (2016).
4. J., Secker, F., Franceschini, S., Ray, “Accident Tolerant Fuel and Resulting Fuel Efficiency Improvements,” *Advances in Nuclear Fuel Management V (ANFM)*, Hilton Head Island, South Carolina, USA, March 29 – April 1 (2015).
5. S., Ray, E., Lahoda, F., Franceschini, “Assessment of Different Materials for Meeting the Requirement of Future Fuel Designs,” *2012 Reactor Fuel Performance Meeting*, Manchester, UK (2012).
6. K. J., Geelhood, W. G., Luscher, P. A., Raynaud, I. E., Porter, “FRAPCON-4.0: A Computer Code for the Calculation of Steady-State, Thermal-Mechanical Behavior of Oxide Fuel Rods for High Burnup,” Pacific *Northwest National Laboratory (PNNL)*, U.S. Department of Energy (DOE) (2015).
7. K. D., Johnson, A. M., Raftery, D. A., Lopes, J., Wallenius, “Fabrication and Microstructural Analysis of UN-U_3Si_2 Composites for Accident Tolerant Fuel Applications,” *Journal of Nuclear Materials*, **vol. 477**, pp. 18–23 (2016).

8. K. E., Metzger, T. W., Knight, R. L., Williamson, "Model of U_3Si_2 Fuel System using BISON Fuel Code," *ICAPP 2014*, Charlotte, NC, USA, Apr. 6–9 (2014).
9. M., Suzuki, H., Saitou, Y., Udagawa, F., Nagase, "Light Water Reactor Fuel Analysis Code: FEMAXI-7; Model and Structure," *Japan Atomic Energy Research Institute (JAEA)* (2013).
10. J. T., White, A. T., Nelson, J. T., Dunwoody, D. D., Byler, D. J., Safarik, K. J., McClellan, "Thermophysical Properties of U_3Si_2 to 1773K," *Journal of Nuclear materials*, **vol. 464**, pp. 275–280 (2015).
11. J. D., Hales, S. R., Novascone, G., Pastore, D. M., Pe, "BISON Theory Manual—The Equations behind Nuclear Fuel Analysis," *Idaho National Laboratory (INL)*, INL/EXT-13-29930 Rev. 2, September 2015 (2015).
12. J. E., Matos, J. L., Snelgrove, "Research Reactor Core Conversion Guidebook-Vol 4: Fuels (Appendices I-K)," *Technical Report*, IAEA-TECDOC- 643 (1992).
13. M. R., Finlay, G. L., Hofman, and J. L., Snelgrove. "Irradiation Behaviour of Uranium Silicide Compounds," *Journal of Nuclear Materials*, **vol. 325**, Issues 2–3, pp.118–128 (2004).
14. G., Pastore, L., Luzzi, V., DiMarcello, P., Van Uffelen, "Physics-based Modeling of Fission Gas Swelling and Release in UO_2 Applied to Integral Fuel Rod Analysis," *Nuclear Engineering and Design*, **vol. 256**, pp. 75–86 (2013).
15. R. L., Williamson, J. D., Hales, S. R., Novascone, M. R., Tonks, D. R., Gaston, C. J., Permann, R. C., Martineau, "Multidimensional Multiphysics Simulation of Nuclear Fuel Behavior," *Journal of Nuclear Materials*, **vol. 423,** Issues 1–3, pp. 149–163 (2012).
16. M. R., Tonks, D., Gaston, P. C., Millett, D., Andrs, P., Talbot, "An Object-oriented Finite Element Framework for Multiphysics Phase Field Simulations," *Computational Materials Science,* **vol. 51**, Issue 1, pp. 20–29 (2012).
17. D., Gaston, C., Newman, G., Hansen, D. L., Grandié, "MOOSE: A Parallel Computational Framework for Coupled Systems of Nonlinear Equations," *Nuclear Engineering and Design,* **vol. 239**, Issue 10, pp. 1768–1778 (2009).